Langmuir

Article

pubs.acs.org/Langmuir

Highly Transparent, Conductive, Flexible Resin Films Embedded with Silver Nanowires

Yaqiu Jiang,[#] Jun Xi, Zhaoxin Wu,*[,#] Hua Dong, Zhixu Zhao, Bo Jiao, and Xun Hou

Key Laboratory of Photonics Technology for Information, Department of Electronic Science and technology, School of Electronic and Information Engineering, Xi'an Jiaotong University, Xi'an 710049, PR China

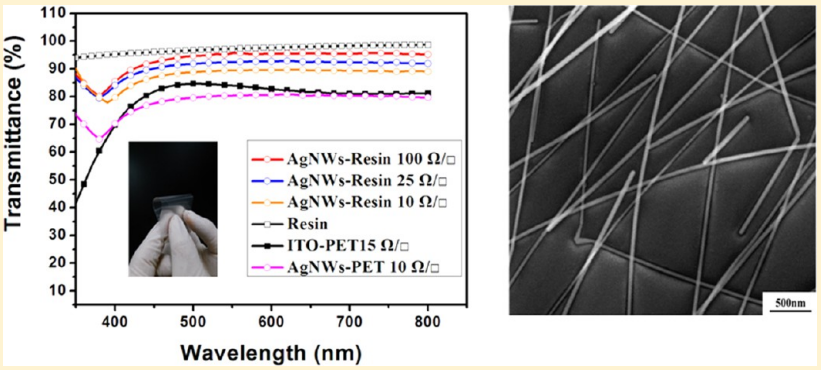

ABSTRACT: In this article, a low sheet resistance and highly transparent silver nanowire (AgNW) resin composite film was demonstrated, which was prepared by a simple and efficacious two-step spin-coating method. By burying the AgNWs below the surface of the transparent resin matrix which was cured at 150 °C in air, we achieved a uniform, highly transparent, conductive, flexible film. Compared to the reported transparent electrodes, this composite transparent and conductive film showed 10 Ω/□ sheet resistance and nearly 90% mean optical transmittance over the UV−visible range simultaneously. Undergoing hundreds of cycles of tensile and compression folding, the composite film slightly increased its sheet resistance by less than 5%, displaying good electromechanical flexibility. These characteristics of the composite AgNW-resin films were expected to be used in applications of flexible optoelectronics.

1. INTRODUCTION

Recently, as flexible and plastic devices have been realized in our life, wearable electronic devices will be quite popular in the future,[1−3] and the growing demand for new transparent electrodes is quite urgent. Indium tin oxide (ITO) electrodes are the most traditional applications in various areas.[4−6] However, the deficiencies of this type of electrode are obvious, such as the rarity of indium and the brittleness of ITO. Therefore, the development of highly transparent flexible electrodes of low resistance is widely required as the replacement for ITO, which can serve as organic light-emitting devices (OLEDs), thin film solar cells, and other organic electric devices. Great efforts have been made to develop new flexible transparent conductors, such as conductive polymers,[7−9] carbon nanotubes (CNT),[10−12] graphenes,[13] random networks of metal nanowires,[14] and mesh structures of self-assembled metallic nanoparticles.[15] Among them, random networks of metal nanowires are promising candidates for their high conductivity and optical transmittance.[16] Silver nanowires have attracted a great deal of attention for their intriguing electrical, thermal, and optical properties. Also, because of their optimal performance with respect to conductivity, silver nanowires (AgNWs) are considered to be very promising candidates in flexible electronics.

The initial development of the AgNW electrodes was based on a rigid substrate. Lee et al. reported solution-processed transparent electrodes consisting of random meshes of AgNWs on a glass substrate.[17] Although the electrode had good conductivity and high optical transmittance, the surface roughness was high, which could create defects across the semiconductor films. Furthermore, the AgNWs were exposed to air, which made them easy to remove and oxidize. To improve the adhesion of AgNWs on substrates, Zhu et al. used a titanium dioxide (TiO_2) sol−gel solution and a poly(3,4-ethylenedioxythiophene)/poly(styrenesulfonate) (PEDOT:PSS) solution to treat AgNWs on glass.[18] Although the AgNW-TiO_2-PEDOT:PSS composites exhibited excellent mechanical properties, the surface roughness of the electrode was still high. Moreover, the substrate they used was glass, which made the electrode inflexible. Then Hu et al. proposed a new kind of AgNW film which was based on poly(ethylene terephthalate) (PET).[19] The transmittance spectrum of that film was much flatter than that for ITO in the visible and near-infrared ranges. Though the root mean square of surface roughness (rms) decreased to 47 nm, it was still too rough for

Received: January 30, 2015
Revised: March 24, 2015
Published: April 13, 2015

DOI: 10.1021/acs.langmuir.5b00384
Langmuir 2015, 31, 4950−4957

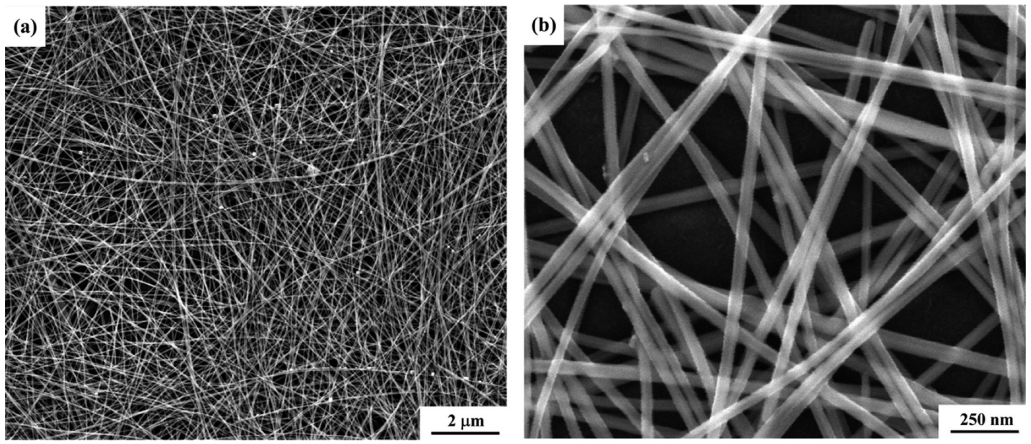

Figure 1. (a) Low- and (b) high-magnification SEM images of the synthesized AgNWs. The AgNWs had a high aspect ratio, and the statistics of the length and diameter of AgNWs were 15−30 μm and 25−35 nm, respectively.

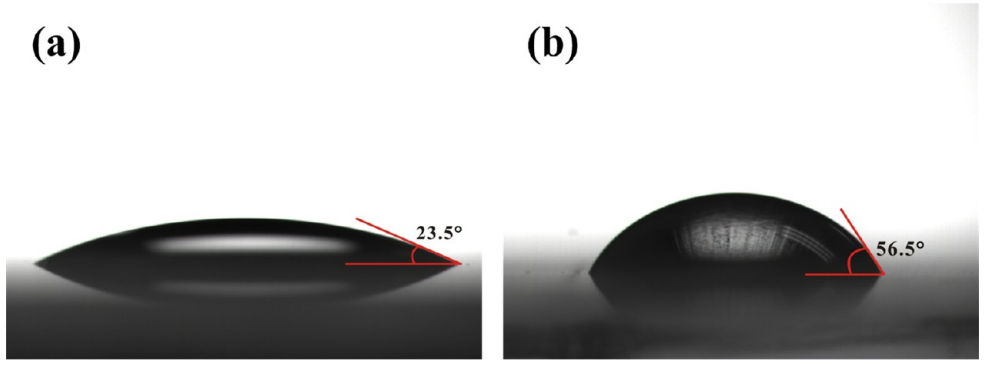

Figure 2. Shapes of the mixed resin droplet on the glass substrate and the PTFE substrate, respectively. (a) The resin contact angle (CA_{glass}) on the glass substrate was 23.73°. (b) The resin contact angle (CA_{PTFE}) on the PTFE substrate was 56.74°.

OLEDs. And the AgNW films based on the PET substrates were only bendable and hardly full flexible. To achieve a smooth, flexible, transparent, conductive AgNW film, Zeng et al. embedded AgNWs in a thick film of poly(vinyl alcohol).[20] This method ensured that the exposed nanowires were flush with the top of the film, thus providing a planar surface on which to deposit more layers. However, the AgNW-PVA film could not meet the requirements of the transparency and sheet resistance simultaneously. For example, when the optical transmission of the AgNW-PVA film reached 87.5% (at 550 nm), the sheet resistance of the AgNW-PVA film was still 63 Ω/□.

For the aim of producing transparent, conductive, flexible films, herein we investigated an alternative method to overcome high surface roughness, high sheet resistance, and low optical transmittance. First we synthesized AgNWs with high aspect ratios as the basis of the transparent electrode's performance. Then AgNWs were spin-coated onto the PTFE (polytetrafluoroethene) substrate. After a facile pressing and heating process, the conductivity of AgNWs was improved. And then the mixed resin was spin-coated onto the predeposited AgNW network. Finally, the composite AgNW-resin film was peeled off of the PTFE substrate after the annealing. The optimized composite AgNW-resin film showed 10 Ω/□ square resistance and 89.96% mean optical transmittance over the UV−visible range simultaneously.

2. METHODS AND EXPERIMENTAL SECTION

2.1. Synthesis of AgNWs and a AgNW Suspension. The air-assisted polyol method was used to synthesize the AgNWs.[21,22] In this synthesis, 10 mL of an ethylene glycol (EG) solution (0.6 M) of poly(vinylpyrrolidone) (PVP) and 0.2 mL of an EG solution of NaCl (0.032 M) were injected into a three-necked round-bottomed flask, which was equipped with a thermocontroller and a magnetic bar. 198 °C was needed to heat the flask for 20 min and should be maintained for another 20 min. Air was pumped continuously into the mixed solution during the whole treatment. Then, we used the centrifugation method to separate the AgNWs. The concentration of AgNWs was titrated by the Volhard method. We demonstrated the SEM images and the statistics of the length and diameter of AgNWs in Figure 1.

2.2. Preparation of the Mixed Resin. The resin we used in the processing of the composite AgNW-resin films was a mixture of five organic reagents: thermoplastic acrylic resin was used as the matrix to form the film because of its high optical transparency, and it had a weight-averaged molecular weight (M_w) of 97 500; ethylene glycol (Sigma-Aldrich) was used as an addictive solvent; ethylene glycol monobutyl ether acetate (Sigma-Aldrich) was a coalescing aid for the resin; dioctyl phthalate was used as plasticizer which aided film formation; and oleamide (Sigma-Aldrich) served as a mold release agent to make the film easy to peel off. Thermoplastic acrylic resin (10 g, 0.102 mmol), ethylene glycol (3 g, 25.5 mmol), ethylene glycol monobutyl ether acetate (3 g, 14.3 mmol), dioctyl phthalate (0.5 g, 0.5 mmol), and oleamide (0.5 g, 0.7 mmol) were placed in sequence into the beaker, which was equipped with a magnetic stirring bar. The mixed solution was stirred for 8 h. Then the mixed resin was achieved.

2.3. Fabrication of the Composite AgNW-Resin Film. We chose PTFE rather than conventional glass as the substrate on which to fabricate the composite AgNW-resin film. A drop of the mixed resin

DOI: 10.1021/acs.langmuir.5b00384
Langmuir 2015, 31, 4950−4957

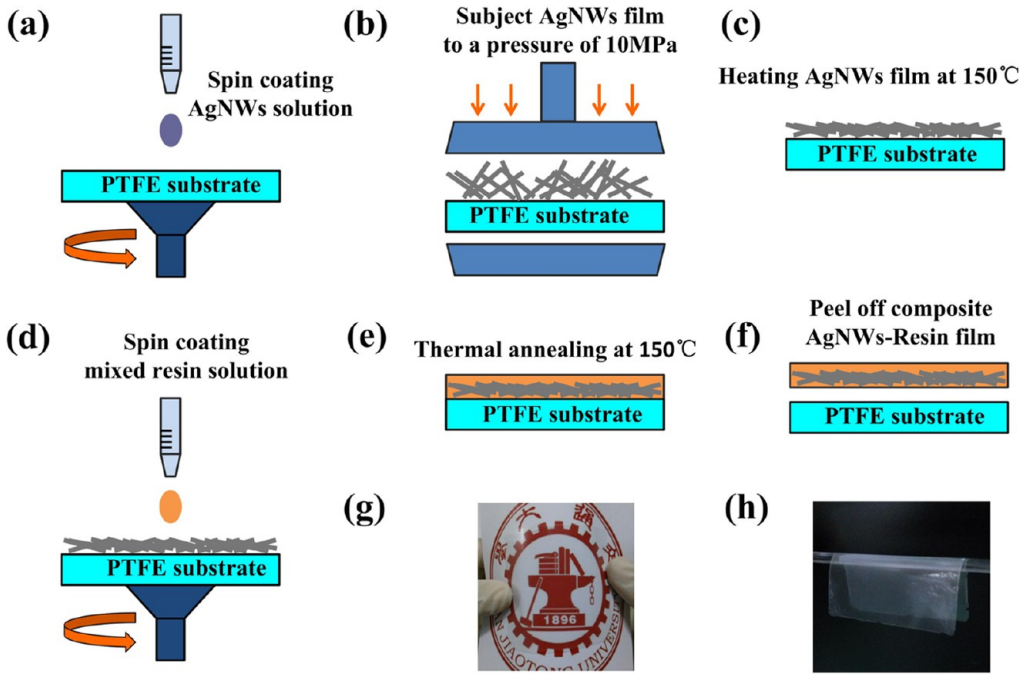

Figure 3. (a–f) Schematic diagram of the procedures for fabricating the composite AgNW-resin film. (g, h) Photographs of the composite AgNW-resin film.

was placed on the glass substrate and PTFE substrate as shown in Figure 2. Because the surface energy of the glass substrate was higher than that of the PTFE substrate, we could find that the resin contact angle (CA_{glass}) on the glass substrate of 23.73° was larger than the CA_{PTFE} (56.74°) on the PTFE substrate. This indicated that the resin droplet spread at the glass substrate more easily than did the PTFE substrate, and the adhesion between the mixed resin film and the glass substrate was stronger than that between the mixed resin film and the PTFE substrate. As the result, peeling the cured resin film off of the PTFE substrate could be much easier than peeling it off of the glass substrate. So we chose the PTFE as the substrate to make sure that the composite AgNW-resin film can be easily peeled off. A AgNW solution was spin-coated at a speed of 1000 rpm for 60 s onto cleaned 400-μm-thick PTFE substrates (7 × 7 cm^2) to form a randomly dispersed AgNW network as shown in Figure 3a. Then the air-dried AgNW film was subjected to a pressure of 10 MPa for 5 s, which is illustrated in Figure 3b. As Figure 3c shows, the pressed AgNW film was held at 150 °C for 15 min in air. Then the mixed resin was sequentially spun at a speed of 600 rpm for 30 s onto the AgNW network, which was also followed by thermal annealing at 150 °C for 10 min. These two processes are indicated in Figure 3d,e. Then the cured resin matrix together with all AgNWs was peeled off of the PTFE substrate, which is shown in Figure 3f.

2.4. Characterization of the Composite AgNW-Resin Films. The morphology of the AgNWs was investigated by scanning electron microscopy (SEM; Quanta 250, FEI) and transmission electron microscopy (TEM; 2100, JEOL). Atomic force microscopy (AFM) (NT-MDT solver P47H-PRO, Russia) was used to characterize the surface roughness of the films. The surface and mesh structures of the composite AgNW-resin films were examined by scanning electron microscopy (SEM; FEI Quanta 250) in high-vacuum mode at 15 kV. Optical transmission spectra of the composite AgNW-resin film was recorded using a UV–vis–NIR spectrometer (Hitachi U-3010, Japan). Sheet resistance measurements were taken using the four-probe tester (M3, Suzhou Jingge Electronic Co. Ltd., China).

3. RESULTS AND DISCUSSION

3.1. Morphology of AgNWs and the Composite AgNW-Resin Films. Figures 1 and 4 show the initial AgNWs as the raw materials of the film. It could be seen that

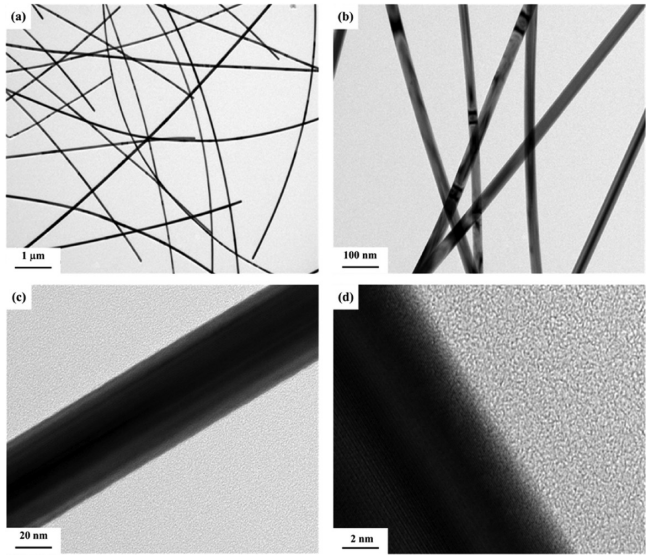

Figure 4. Low- and high-magnification TEM images of the synthesized AgNWs.

after being separated by centrifugation and washed with ethanol and deionized water that almost no PVP adsorbed on the surface of AgNWs. Also, AgNWs with a high aspect ratio were synthesized, and the statistics of the diameter and length of AgNWs were 25–35 nm and 15–30 μm, respectively. All of the results served to improve the AgNW conductivity.

Before the AgNW film was heated and covered with the mixed resin, the stamping process was needed as the preliminary treatment. This strategy of mechanical pressing could not only effectively increase the connection of the AgNW mesh and decrease the sheet resistance but also could greatly improve the film morphology.[19,23] When the AgNWs were spun onto the PTFE substrate, AgNWs were all connected loosely (Figure 5a). Therefore AgNW films were subjected to a

DOI: 10.1021/acs.langmuir.5b00384
Langmuir 2015, 31, 4950–4957

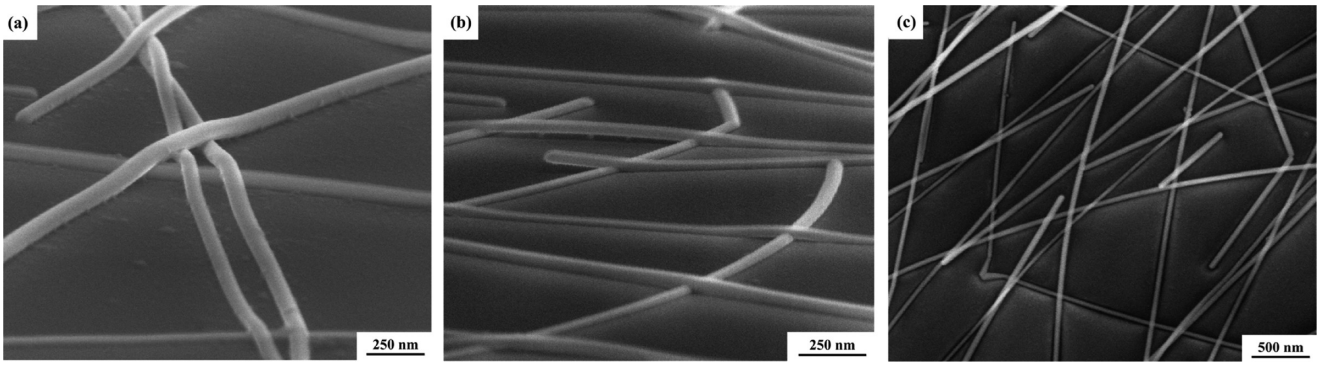

Figure 5. (a) SEM image of the unpressed AgNW film with a sheet resistance of 6.2×10^3 Ω/□. Weak connections of the AgNWs could be observed in the off-angle view. (b) SEM images of the AgNW films pressed at 10 MPa for 5 s, having a sheet resistance of 30 Ω/□. AgNWs connecting tightly could be observed in the off-angle view. (c) Top view of the SEM images of the surface of the composite AgNW-resin film (10 Ω/□). The tightly connected AgNWs were buried in the mixed-resin matrix and were flush with the top of the film.

pressure of 10 MPa for 5 s, and as shown in Figure 5b, the compressed connection points could obviously be seen from the off-angle view. After the films were pressed, the sheet resistance was decreased distinctly. Table 1 shows the change in the resistance before and after pressing.

Table 1. Comparison of the Sheet Resistance between Unpressed and Pressed AgNW Films

speed of spin coating (rpm)	unpressed (Ω/□)	pressed (Ω/□)
1000	6.2×10^3	30
2000	9.7×10^3	72
3000	1.6×10^4	150

Although the stamping process could make AgNWs connect tightly, there were still some weak connections among AgNWs. So the pressed AgNW film was then held at 150 °C for 15 min in air to make the AgNWs melt and fuse at the junctions.[17,24−26] The sheet resistance of the composite AgNW-resin film decreased from 30 to 10 Ω/□ because of the increasing contact area between the AgNWs.

The top-view SEM image (Figure 5c) showed the surface of the composite AgNW-resin film with a sheet resistance of 10 Ω/□. The AgNWs formed a uniform mesh without significant nanowire density differences across the substrate, and the predeposited AgNW mesh was buried in the surface of the resin matrix. The surface topography of the composite AgNW-resin film, examined by atomic force microscopy (AFM), is shown in Figure 6. Here we used the bare AgNW mesh which was spin-coated onto the clean glass substrate as the reference, and the AFM topographical image of the bare AgNW mesh is also shown in Figure 6. Figure 6a,c revealed a dense network of randomly oriented bare AgNWs, and the presence of protruding AgNWs led to localized height elevations greater than 150 nm (Figure 6b). On the contrary, the surface topography of the composite AgNW-resin film described herein appeared to be very smooth in Figure 6d,f, and the height variation in the 20×20 μm^2 scanned area was less than 15 nm (Figure 6e). The bare AgNWs coating the glass substrate and

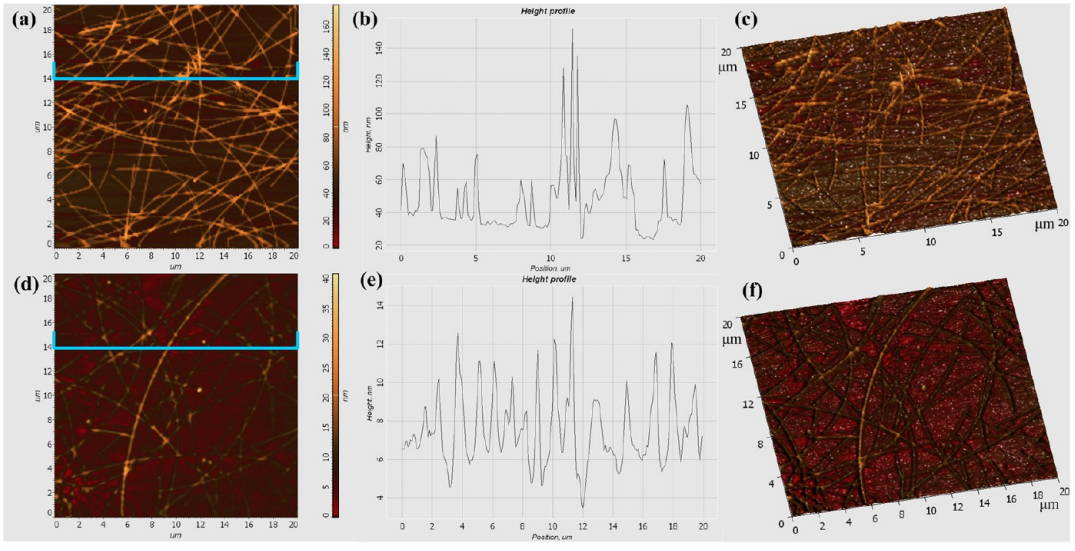

Figure 6. AFM topological images of bare AgNWs deposited on the glass substrate and the composite AgNW-resin film. (a, b) 2D morphology images, section curves, and roughness of bare AgNWs coating the glass substrate. (c) 3D AFM topological images of bare AgNWs deposited on the glass substrate. (d) AFM image (2D) of the composite AgNW-resin film surface. (e) AFM height line profile of the composite AgNW-resin film surface. (f) Tapping-mode AFM scan (3D) of the composite AgNW-resin film surface. The scan area was 20×20 μm^2.

DOI: 10.1021/acs.langmuir.5b00384
Langmuir 2015, 31, 4950−4957

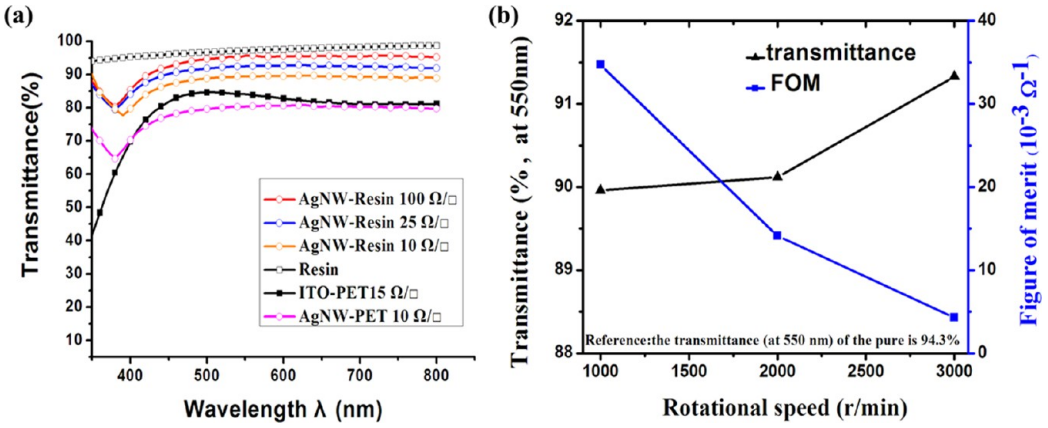

Figure 7. (a) Optical transmittance of the composite AgNW-resin films with different sheet resistances, the mixed resin film (16 μm), ITO-PET (100 μm), and AgNW-PET (100 μm) measured with a UV−vis−NIR spectrometer. (b) FOM values of the composite AgNW-resin film vs the spin-coating speed for a AgNW solution.

Figure 8. Photographs of the composite AgNW-resin film under different backgrounds. (a) Photograph of the composite AgNW-resin film under a brown background; the transparent film exhibited a transparency of 89.96% and a sheet resistance of 10 Ω/□. The sheet resistance distribution of the composite AgNW-resin film was uniform, and the sheet resistance at different points are as follows: A = 9.96 Ω/□, B = 10.8 Ω/□, C = 10.2 Ω/□, D = 9.8 Ω/□, and E = 10 Ω/□. (b, c) Photographs of the composite AgNW-resin film against a white background. The composite AgNW-resin film had high transparency and flexibility.

the composite AgNW-resin film have root-mean-square surface roughness (rms) values of 22 and 2.2 nm, respectively. Accordingly, the mechanical pressing and heating not only increased the conductance but also greatly improved the film morphology. Meanwhile, the applied liquid monomer penetrated the AgNW network during the formation of the mixed resin substrate, filling the openings between AgNWs and the space unoccupied by AgNWs at the PTFE interface. A highly cross-linked polymer network was formed by the subsequent polymerization and buried most of the AgNWs with the exception of those that were in contact with the PTFE surface.

3.2. Optoelectronic Properties and Sheet Resistance of the Composite AgNW-Resin Films. The important property of transparent and conductive films was optical transmittance over a broad range of wavelength.[17,27] The transmittance spectra of three kinds of films (an ITO film magnetron sputtered on PET (thickness 100 μm), a AgNW film deposited on PET (thickness 100 μm), and the composite AgNW-resin film (thickness 16 μm)) were obtained and are shown in Figure 7a. The absorption of light by the pure resin (or PET substrate) itself was not excluded when we obtained the transmittance spectra of these three kinds of films. We also applied three different rotational speeds (1000, 2000, and 3000 rpm) to spin-coat the AgNW solution while we maintained the conditions for other steps of fabricating the composite AgNW-resin film unchanged. The transmittance and sheet resistance of these three composite AgNW-resin films were also different. Compared to the mixed resin film (16 μm) with a transmittance of 94.3%, the optical transmittance of the composite AgNW-resin film at 550 nm reached 91.33% when the sheet resistance was 100 Ω/□. When the optical transmittance values of the composite AgNW-resin film were 90.12 and 89.96%, the sheet resistances were 25 and 10 Ω/□, respectively. An ITO film magnetron sputtered on PET (ITO-PET) and a AgNW film deposited on PET (AgNW-PET) were prepared and used as a reference. When ITO-PET had the same resistance as the composite AgNW-resin film, the transparency in the visible range was lower than that of the composite AgNW-resin film. More importantly, the transparency of the composite AgNW-resin film was high and constant in the near-infrared regions, which was quite beneficial to solar cells.

Furthermore, to use a transparent film in flexible electronics applications, key prerequisites were not only high transmittance and low sheet resistance but also low haze. The transmittance haze represented the percentage of light diffusely scattered compared to the total light transmitted[28,29] and was defined as $(T_d/T_t) \times 100$, where T_d is diffuse transmittance and T_t is total transmittance. The diffuse transmittance occurred because of the light scattering from surface irregularities such as roughness

DOI: 10.1021/acs.langmuir.5b00384
Langmuir 2015, 31, 4950−4957

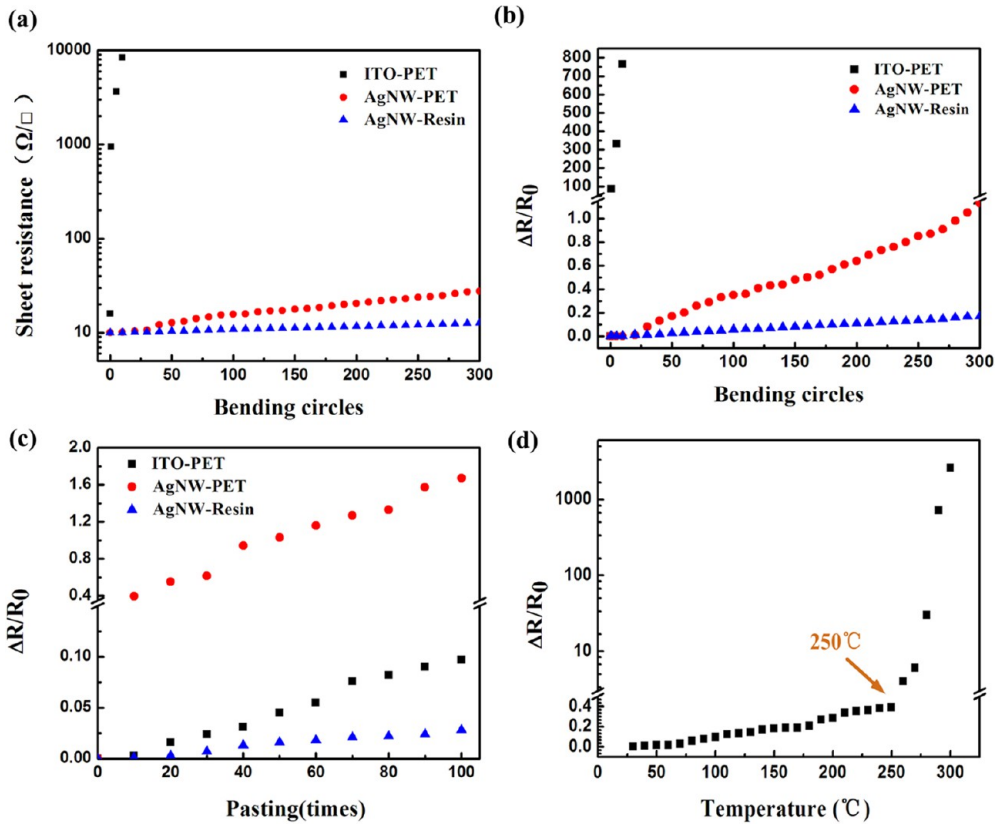

Figure 9. (a) Sheet resistance vs bending times for ITO-PET (100 μm), AgNW-PET (100 μm), and the composite AgNW-resin (16 μm). (b) Increase in the sheet resistance of ITO-PET, AgNW-PET, and composite AgNW-resin films as a function of the number of cycles after repeated tensile bending. (c) Variation of sheet resistance values of ITO-PET (100 μm), AgNW-PET (100 μm), and composite AgNW-resin films (16 μm) as a function of the pasting times. (d) Evolution of the resistance of the composite AgNW-resin film with increasing temperature in air.

and particles on a sample. We also measured the haze of the composite AgNW-resin films which were fabricated at three different rotational speeds (1000, 2000, and 3000 rpm), and the haze values of the composite AgNW-resin films were in the range of 1.1−3.8%. We found that the haze of the composite AgNW-resin film increased with decreasing rotational speed. Because the density of AgNWs increased, more light was scattered. Thus, the composite AgNW-resin film presented comparable haze to ITO-PET (5.2%).

To determine the optimum performance of the composite AgNW-resin film, we calculated the value of the figure of merit (FOM). The FOM was based on the sheet resistance (R_s) and optical transmittance (T) at a wavelength of 550 nm and was defined as FOM = T^{10}/R_s.[30] Figure 7b shows the optical transmittance and FOM values of the composite AgNW-resin film. We found that the FOM of the composite AgNW-resin film increased significantly with decreasing rotational speed. Because the density of AgNWs increased, the sheet resistance of the AgNW-resin film dramatically decreased with decreasing rotational speed. When the rotational speed reached 3000 rpm, the composite AgNW-resin film showed the lowest FOM value of 4.04×10^{-3} Ω^{-1}, and when the rotational speed reached 1000 rpm, the composite AgNW-resin film had the highest FOM value of 34.71×10^{-3} Ω^{-1}, which achieved a balance between the low sheet resistance and the high optical transmittance.

A uniform composite AgNW-resin film (16 μm) of large scale (7×7 cm^2) is shown in Figure 8a. Figure 8b,c shows the composite AgNW-resin film with high transparency and flexibility. We have great confidence that it will be quite popular in the optoelectronics industry in the future.

3.3. Mechanical Properties and Thermal Stability of the Composite AgNW-Resin Films. Burying the AgNW film at the surface of the resin matrix had a great advantage over other transparent films in the aspect of mechanical robustness against adhesion and bending. The composite AgNW-resin film (16 μm) was compared to ITO-PET and AgNW-PET. The flexibility of these three films was evaluated by a bending test with a radius of curvature of 2 mm, and the changes in the sheet resistance of three films with increasing bending times are shown in Figure 9a,b.

It was unsurprising that the ITO film cracked and its resistance increased by a factor of 10 after only five cycles of tensile folding, which exhibited the poor stability. The AgNW-PET film had better performance, and its resistance increased 2-fold after 250 cycles of tensile folding. However, the resistance of the composite AgNW-resin film increased only 10% after 250 cycles of tensile folding. This small increase in resistance was attributed to the failed electrical contacts between AgNWs. Obviously, the result indicated that the composite AgNW-resin film was better than ITO-PET and AgNW-PET. The result was also comparable to that of PEDOT:PSS,[7] CNT,[10−12] and graphene films.[13]

The mechanical tape tests were also executed to examine the adhesion of the AgNWs to the substrate. Here we pressed 3M tape (ScotchMagic Tape) under a pressure of approximately 2 MPa for 30 s. ITO-PET and AgNW-PET were used as

DOI: 10.1021/acs.langmuir.5b00384
Langmuir 2015, 31, 4950−4957

references to illustrate the excellent properties of the composite AgNW-resin film.

From Figure 9c we noted that after being pasted 40 times the $\Delta R/R_0$ ($\Delta R = R - R_0$) of the AgNW-PET film reached nearly 100%, the $\Delta R/R_0$ of the ITO-PET film reached about 3%, and the $\Delta R/R_0$ of the composite AgNW-resin film reached only 1%. When the pasting times became 100, the $\Delta R/R_0$ of the AgNW-PET film reached as high as 170%, which meant that most of the AgNWs were peeled off of the PET substrate. The $\Delta R/R_0$ of the ITO-PET film grew to 10%, and the $\Delta R/R_0$ of the composite AgNW-resin films changed to only 2.5%. This excellent mechanical adhesion arose from the special structure in Figure 10a, where all of the AgNWs were firmly anchored by

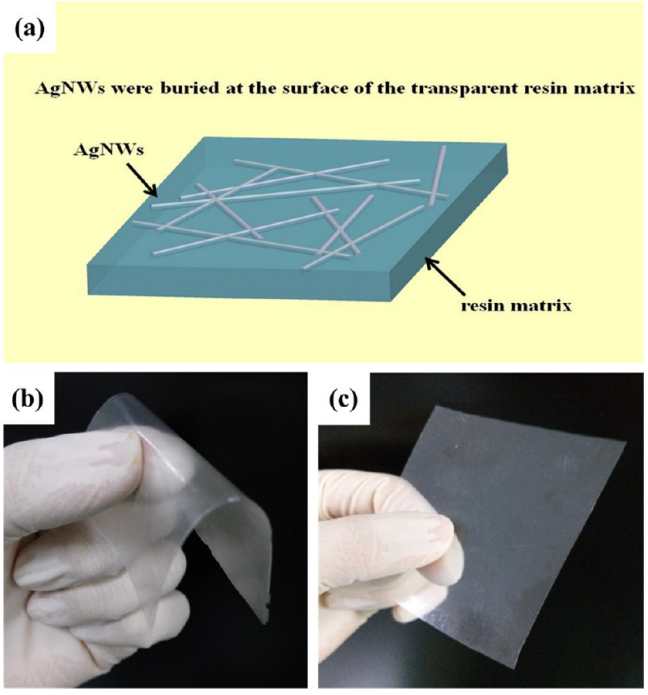

Figure 10. (a) Structure of the composite AgNW-resin films. AgNWs were buried in the mixed resin matrix. (b, c) Holding the composite AgNW-resin film (16 μm) and AgNW-PET film (100 μm) in hand, respectively. (b) The flexible composite AgNW-resin film exhibited high flexibility and bent naturally to maintain the natural curve. (c) AgNW-PET could not bend naturally and exhibited low flexibility.

the resin matrix. Figure 10b shows that the composite AgNW-resin film (16 μm) was fully flexible and bent naturally to maintain the natural curve but the AgNWs film coated onto the PET substrate (100 μm) was hardly fully flexible and could not bend naturally (Figure 10c).

We further tested the thermal stability of the composite AgNW-resin film with the sheet resistance of 10 Ω/□. As shown in Figure 9d, $\Delta R/R_0$ increased slowly up to nearly 40% at 250 °C, which probably originated from the relatively high thermal expansion of the resin matrix. And the composite AgNW-resin film maintained a considerable thermal stability before 250 °C, above which oxidation led to a rapid increase in the sheet resistance. So we could conclude that the maximum operating temperature of the composite AgNW-resin films was nearly 250 °C. As a comparison, the resistance of AgNW films on Si was reported to have an obvious increase when the AgNW film was annealed in air at 200 °C for 1 h.[17] This also prove that burying AgNWs at the surface of the mixed resin could improve the thermal stability of the AgNW film.

We also compared our composite AgNW-resin film to different types of transparent films; the numbers are listed in Table 2. From Table 2, we concluded that though selected

Table 2. Comparison of the Sheet Resistance and the Optical Transmittance between the Reported Transparent AgNW Films and the Composite AgNW-Resin Film

structure	sheet resistance (Ω/□)	transmittance (%)	references
AgNW-PET film	8.6	60	23
AgNW/ITO-NP film	11	85.3	31
AgNW-PVA film	63	87.5	20
AgNW/PEDOT:PSS film	10.76	84.3	32
ITO NP/Ag NW/ITO NP film	20	80	19
AgNW- acrylate film	12	82	33
composite AgNW-resin film	10	89.96	ours

research groups had proposed different kinds of creative strategies for fabricating AgNW composite films, the nanowire mesh still contained the weak properties. Low sheet resistance and high transmittance could not be obtained in these transparent conductive films simultaneously. When the sheet resistance reached 8.6 Ω/□, the transmittance was as low as 60%.[23] Meanwhile, because the transmittance of the film was high, the sheet resistance could reach 63 Ω/□, which hindered its application in industry. Fewer AgNWs were needed to achieve the comparably low sheet resistance in the composite AgNW-resin film because AgNWs with a high aspect ratio were synthesized and the facile pressing and heating process was adopted in the experiment. Therefore, the performance of the composite AgNW-resin film could be improved. Consequently, the composite AgNW-resin film exhibited not only high transmittance (89.96%) but also low sheet resistance (10 Ω/□). With the unique high performance as well as full flexibility, this new approach might boost large-scale applications of the composite AgNW-resin film in flexible, plastic, and wearable optoelectronic devices.

4. CONCLUSIONS

A typical flexible, transparent, conducting film of AgNWs was developed by burying a AgNW film below the surface of a transparent resin matrix. Studies showed that the composite AgNW-resin film had superior mechanical robustness and ultralow surface roughness. Appropriate mechanical pressing could decrease the composite AgNW-resin films' sheet resistance to a value of 10 Ω/□ while maintaining an optical transmittance of as high as 90%. Electromechanical testing demonstrated that for more than 100 bending cycles the composite AgNW-resin film was extremely stable, with the variation in sheet resistance being less than 2.5%. Because the transparence of the composite AgNW-resin film was 89.96% and constant in the near-infrared region, this was quite beneficial to solar cells. Therefore, we expected that this work could be helpful for the development of high-quality wearable and flexible optoelectronic devices.

■ AUTHOR INFORMATION

Corresponding Author

*E-mail: zhaoxinwu@mail.xjtu.edu.cn.

DOI: 10.1021/acs.langmuir.5b00384
Langmuir 2015, 31, 4950−4957

Author Contributions

[#]Y.J. and Z.W. equally contributed to this work.

Notes

The authors declare no competing financial interest.

■ ACKNOWLEDGMENTS

This work was financially supported by the Basic Research Program of China (2013CB328705), the National Natural Science Foundation of China (grant nos. 61275034 and 61106123), Foundation of the Ministry of Education of the China Ph.D. programs (grant no. 20130201110065), and Fundamental Research Funds for the Central Universities (grant no. xjj2012087).

■ REFERENCES

(1) Lewis, B. G.; Paine, D. C. Applications and processing of transparent conducting oxides. *MRS Bull.* **2000**, *25*, 22−27.
(2) Minami, T. Transparent conducting oxide semiconductors for transparent electrodes. *Semicond. Sci. Technol.* **2005**, *20*, S35−S44.
(3) Wu, Z. C.; Chen, Z. H.; Du, X.; Logan, J. M.; Sippel, J.; Nikolou, M.; Kamaras, K.; Reynolds, J. R.; Tanner, D. B.; Hebard, A. F.; Rinzler, A. G. Transparent, conductive carbon nanotube films. *Science* **2004**, *305*, 1273−1276.
(4) Ishibashi, S.; Higuchi, Y.; Ota, Y.; Nakamura, K. Low resistivity indium−tin oxide transparent conductive films 0.1. Effect of introducing H_2O gas or H_2 gas during direct current magnetron sputtering. *J. Vac. Sci. Technol.* **1990**, *8*, 1399−1402.
(5) Ishibashi, S.; Higuchi, Y.; Ota, Y.; Nakamura, K. Low resistivity indium−tin oxide transparent conductive films 0.2. Effect of sputtering voltage on electrical property of films. *J. Vac. Sci. Technol.* **1990**, *8*, 1403−1406.
(6) Carcia, P. F.; McLean, R. S.; Reilly, M. H.; Li, Z. G.; Pillione, L. J.; Messier, R. F. Low-stress indium−tin−oxide thin films rf magnetron sputtered on polyester substrates. *Appl. Phys. Lett.* **2002**, *81*, 1800−1802.
(7) Lang, U.; Müller, E.; Naujoks, N.; Dual, J. Microscopical investigations of PEDOT: PSS thin films. *Adv. Funct. Mater.* **2009**, *19*, 1215−1220.
(8) Ouyang, J.; Xu, Q.; Chu, C.-W.; Yang, Y.; Li, G.; Shinar, J. On the mechanism of conductivity enhancement in poly(3,4-ethylenedioxythiophene): poly(styrene sulfonate) film through solvent treatment. *Polymer* **2004**, *45*, 8443−8450.
(9) Xia, Y.; Ouyang, J. Salt-induced charge screening and significant conductivity enhancement of conducting poly (3,4-ethylenedioxythiophene) poly (styrenesulfonate). *Macromolecules* **2009**, *42*, 4141−4147.
(10) Kaempgen, M.; Duesberg, G. S.; Roth, S. Transparent carbon nanotube coatings. *Appl. Surf. Sci.* **2005**, *252*, 425−429.
(11) Jung, Y. C.; Shimamoto, D.; Muramatsu, H.; Kim, Y. A.; Hayashi, T.; Terrones, M.; Endo, M. Robust, conducting, and transparent polymer composites using surface-modified and individualized double-walled carbon nanotubes. *Adv. Mater.* **2008**, *20*, 4509−4512.
(12) Gu, H.; Swager, T. M. Fabrication of free-standing, conductive, and transparent carbon nanotube films. *Adv. Mater.* **2008**, *20*, 4433−4437.
(13) Bae, S.; Kim, H.; Lee, Y.; Xu, X.; Park, J. S.; Zheng, Y.; Balakrishnan, J.; Lei, T.; Kim, H. R.; Song, Y. I.; Kim, Y. J.; Kim, K. S.; Ozyilmaz, B.; Ahn, J. H.; Hong, B. H.; Iijima, S. Roll-to-roll production of 30-in. graphene films for transparent electrodes. *Nat. Nanotechnol.* **2010**, *5*, 574−578.
(14) Kang, M.-G.; Kim, M.-S.; Kim, J.; Guo, L. J. Organic solar cells using nanoimprinted transparent metal electrodes. *Adv. Mater.* **2008**, *20*, 4408−4413.
(15) Vakarelski, I. U.; Chan, D. Y. C.; Nonoguchi, T.; Shinto, H.; Higashitani, K. Assembly of gold nanoparticles into microwire networks induced by drying liquid bridges. *Phys. Rev. Lett.* **2009**, *102*, 058303.
(16) Sun, Y. G. Silver nanowires-unique templates for functional nanostructures. *Nanoscale* **2010**, *2*, 1626−1642.
(17) Lee, J. Y.; Connor, S. T.; Cui, Y.; Peumans, P. Solution-processed metal nanowire mesh transparent electrodes. *Nano Lett.* **2008**, *8*, 689−692.
(18) Zhu, R.; Chung, C.-H.; Cha, K. C.; Yang, W.; Zheng, Y. B.; Zhou, H.; Song, T.-B.; Chen, C.-C.; Weiss, P. S.; Li, G.; Yang, Y. Fused silver nanowires with metal oxide nanoparticles and organic polymers for highly transparent conductors. *ACS Nano* **2011**, *5*, 9877−9882.
(19) Hu, L. B.; Kim, H. S.; Lee, J.-Y.; Peter, P.; Yi, C. Scalable coating and properties of transparent, flexible, silver nanowire electrodes. *ACS Nano* **2010**, *4*, 2955−2963.
(20) Zeng, X. Y.; Zhang, Q. K.; Yu, R. M.; Lu, C. Z. A new transparent conductor: silver nanowire film buried at the surface of a transparent polymer. *Adv. Mater.* **2010**, *22*, 4484−4488.
(21) Sun, Y. G.; Xia, Y. N. Large-scale synthesis of uniform silver nanowires through a soft, self-seeding, polyol process. *Adv. Mater.* **2002**, *14*, 833−837.
(22) Tang, X. L.; Tsuji, M.; Jiang, P.; Nishio, M.; Jang, S. M.; Yoon, S. H. Rapid and high-yield synthesis of silver nanowires using air-assisted polyol method with chloride ions. *Colloids Surf., A* **2009**, *338*, 33−39.
(23) Tokuno, T.; Nogi, M.; Karakawa, M.; Jiu, J. T.; Nge, T. T.; Aso, Y.; Suganuma, K. Fabrication of silver nanowire transparent electrodes at room temperature. *Nano Res.* **2011**, *4*, 1215−1222.
(24) Madaria, A. R.; Kumar, A.; Ishikawa, F. N.; Zhou, C. W. Uniform, highly conductive, and patterned transparent films of a percolating silver nanowire network on rigid and flexible substrates using a dry transfer technique. *Nano Res.* **2010**, *3*, 564−573.
(25) Gaynor, W.; Lee, J. Y.; Peumans, P. Fully solution-processed inverted polymer solar cells with laminated nanowire electrodes. *ACS Nano* **2010**, *4*, 30−34.
(26) Lee, J. Y.; Connor, S. T.; Cui, Y.; Peumans, P. Semitransparent organic photovoltaic cells with laminated top electrode. *Nano Lett.* **2010**, *10*, 1276−1279.
(27) De, S.; Higgins, T. M.; Lyons, P. E.; Doherty, E. M.; Nirmalraj, P. N.; Blau, W. J.; Boland, J. J.; Coleman, J. N. Silver nanowire networks as flexible, transparent, conducting films: extremely high DC to optical conductivity ratios. *ACS Nano* **2009**, *3*, 1767−1774.
(28) Raut, H. K.; Ganesh, V. A.; Nair, A. S.; R, S. Anti-reflective coatings: A critical, in-depth review. *Energy Environ. Sci.* **2011**, *4*, 3779−3804.
(29) Lee, C.; Kim, J. J. Enhanced Light Out-Coupling of OLEDs with Low Haze by Inserting Randomly Dispersed Nanopillar Arrays Formed by Lateral Phase Separation of Polymer Blends. *Small* **2013**, *9*, 3858−3863.
(30) Jeong, J. A.; Kim, H. K. Ag nanowire percolating network embedded in indium tin oxide nanoparticles for printable transparent conducting electrodes. *Appl. Phys. Lett.* **2014**, *104*, 071906.
(31) Chung, C. H.; Song, T. B.; Bob, B.; Zhu, R.; Yang, Y. Solution-processed flexible transparent conductors composed of silver nanowire networks embedded in indium tin oxide nanoparticle matrices. *Nano Res.* **2012**, *5*, 805−814.
(32) Choi, D. Y.; Kang, H. W.; Sung, H. J.; Kim, S. S. Annealing-free, flexible silver nanowire-polymer composite electrodes via a continuous two-step spray-coating method. *Nanoscale* **2013**, *5*, 977−983.
(33) Yu, Z. B.; Zhang, Q. W.; Li, L.; Chen, Q.; Niu, X. F.; Liu, J.; Pei, Q. B. Highly flexible silver nanowire electrodes for shape-memory polymer light-emitting diodes. *Adv. Mater.* **2011**, *23*, 664−668.

DOI: 10.1021/acs.langmuir.5b00384
Langmuir 2015, 31, 4950−4957